

Collapse analysis of the Daikai station in Kobe Metropolitan

David Lourenço Brito

Department of Civil Engineering and Architecture, IST, Technical University of Lisbon

1. Introduction

Generally, underground structures are characterized by the absence of important damages when subjected to seismic action.

However, on 17 January 1995, Kobe earthquake occurs and a large part of the stations and underground tunnels have suffered severe damage, including total collapse. One of the Kobe subway stations which raised great interest and research was Daikai station, which suffered a total collapse of its central pillars over a length of 80m, with settlements up to 2.5m at surface. The Kobe earthquake contributed to change the way the scientific community view the vulnerability of these structures.

This work is focused on the analysis of the failure mechanism in Daikai station. Moreover, understand how the influence of the construction process affects the static and dynamic response of the tunnel and the surrounding soil.

The dissertation is divided into six chapters. After the introduction, the second chapter corresponds to a general framework of the Kobe earthquake. It is done a literature review of damage in the underground subway system of Kobe and then more specifically at the station Daikai. The damage evaluated and defined analysis models to the underground station are described. On the third chapter is calibrated the numerical model. The models for studying the phenomenon of wave propagation and cyclic behavior of soils are described. In the fourth chapter numerical linear elastic analysis are conducted to evaluate the mechanism failure of the central columns. Chapter five presents the results of the consideration of construction phasing. A few parameters such as the variation of plastic zones, forces and relative displacements in elements are analyzed. In the last chapter, conclusion remarks and future perspectives are presented.

2. Daikai Station

The Hyogoken--Nanbu earthquake, also known as the "Great Hanshin Earthquake", on 17 January 1995 had an extreme impact on buildings and infrastructure in the Kobe region, with a magnitude of 7.2 on the Richter scale. Kobe is inserted in a zone of converging tectonic plates 4 (Fig. 1), with intense activity. The mechanism of failure was this type "strike slip".

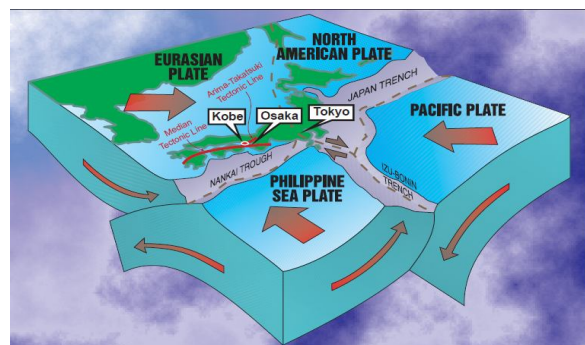


Fig. 1 - Tectonic activity that caused the Kobe earthquake (adapted from Japan, EQ, 1995)

2.1 Damage in the Kobe subway system

More than 6400 people lost their lives during such seismic activity. Was affected not only the region of Kobe, but also Osaka, which together are the second most industrialized and populated after Tokyo.

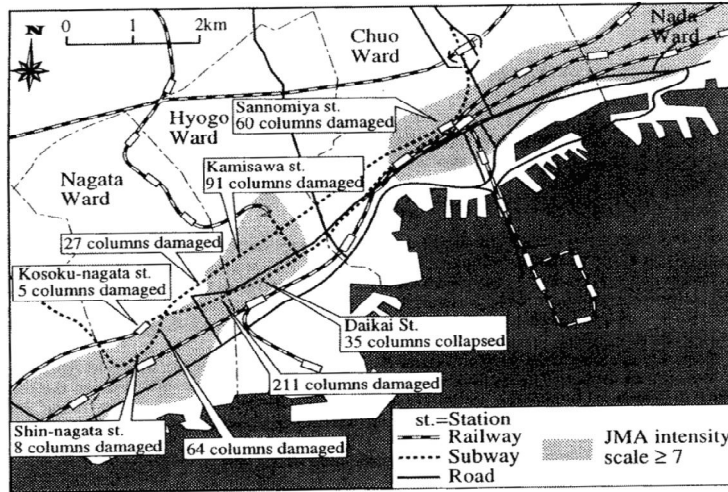


Fig. 2 - Location of damaged subways and damage patterns (adapted from Yoshida and Nakamura, 1996)

As shown in Fig. 2 the level of damage in the region of Kobe was not limited exclusively to the underground system. The remaining roads, such as highways and railway lines were also affected. Most of the damage refers to partial or total collapse of columns of viaducts that held the access structures or formed an integral part of the network traffic.

2.2 Daikai Station

The construction of Daikai station, inserted in middle of "Tozai Line", began in August 1962. The construction process include the total excavation using peripheral walls to support the ground and subsequent construction of the station (*cut-and-cover method*).

Although there is no information on the constructive process for the station, the following approach was adopted, in which it uses two levels of grounding - Fig. 3.

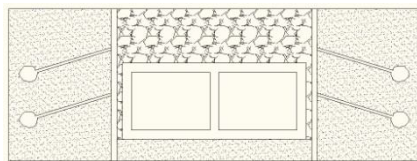


Fig. 3 - Construction process - last phase

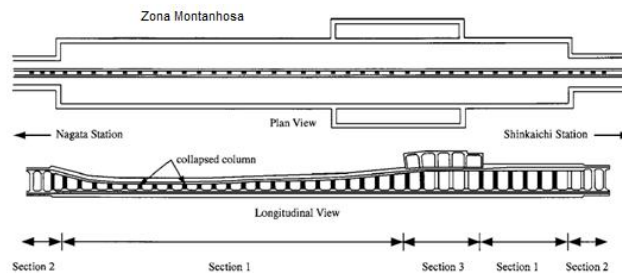
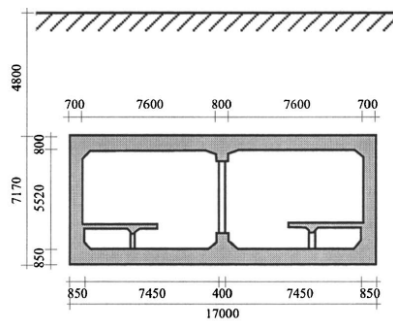


Fig. 4 - Longitudinal damage patterns to the Daikai Station (adapted from Iida et al., 1996)

Longitudinally, the station can be divided into three distinct sections (Fig. 4): (1) the central section collapsed; (2) the section of the tunnel, where most severe damage occurred, and (3) the access zone that has two floors, also without presenting data biggest concern.

The structure consists of two floor section and terminal access by a single floor in the remaining. Denominating the B2 the lower floor, this includes platforms for transportation and rail travel. The top floor will be designated by B1 serving outdoor access by users and control output / input from them. For a single floor section (Fig. 5) landfill overlying layer has a thickness of 4.8 m, whereas in the access zone

are 1.9 meters above the ground structure. The area for the ground floor, which extends longitudinally of 120 m, is basically a rectangular structure with a closed cross section width of 17 m by 7.17 m long.



Round steel bars with diameters from 16 to 25 mm were used as reinforcing for the walls and slabs, and 32 mm diameter bars were used in the central column. A transverse hoop (9 mm diameter) was placed at every 350 mm in the center column.

Fig. 5 - Cross section of the Daikai Station, dimensions in mm (Huo *et al.*, 2005)

2.3 Geological setting at Daikai station

The site of the Daikai station is essentially composed of soft Holocene alluvial deposits and dense Pleistocene gravel, overlain by man-made fill.

The ground water table was located at a depth of 6-8m below the ground surface, which was 3-5m lower than in 1959, prior to the construction of the station. Referring to another source, Kobe city (1980), the soil depth of the base was deep on the west side and it consists of silty or clayey surface soil. It becomes shallow toward east; the depth at the Daikai station site is about 15 m and that at the Shinkaichi station is less than 10 m. In addition, sand becomes more predominant toward east.

2.4 Earthquake induced damages

The central columns collapsed in East area, resulting in significant settlement of the upper slab and the surrounding soil. Many cracks were observed in the longitudinal walls as well as the transverse directions.

Damage was the most severe at section 1 (Fig. 5) in the Nagata side zone. Almost all the center columns completely collapsed and the ceiling slab fell down. As a result, the original box frame structure distorted to an M-shaped section. The ceiling slab kinks and cracks 150 to 250 mm wide appeared in the longitudinal direction about 2.15 to 2.40 m from the center line of the columns. In addition, the separation of cover concrete was observed over the almost entire area near the haunch and the intersection between the ceiling slab and the lateral wall.

In the lateral wall, separation of the cover concrete was observed near both the top and bottom haunches. Diagonal cracks were observed in all the walls in the transverse direction.

2.5 Numerical modelling

To study the dynamic soil structure interaction some simplifications were considered, such as:

- Evaluate a single transverse profile;
- Soil layers are horizontal, not taking into account the variation of longitudinal layers along the tunnel;
- The tunnel is modeled with finite element bar;

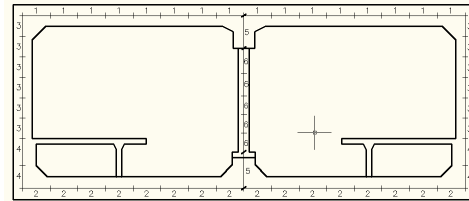
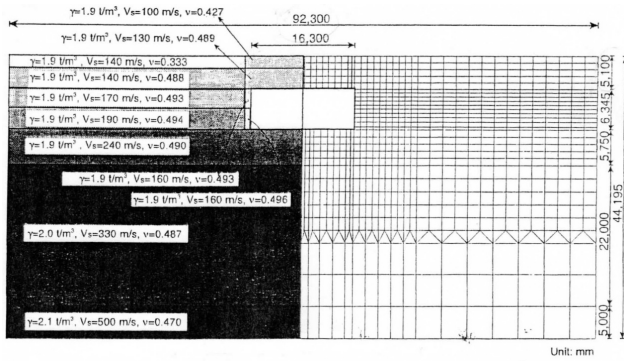


Fig. 6 - Soil-structure system used in the dynamic response analysis (adapted from Yoshida and Nakamura, 1996) **Fig. 7 - Discretization for the station**

At first step, in order to appropriately estimate the dynamic response of structure during the earthquake, dynamic response analysis of the soil-structure was conducted using a finite element method considering the soil discretization above (Fig. 6). It was conducted with the software SAP2000, which only develop elastic linear analysis. In Fig. 7 it's presented the discretization for the station using frame elements. Different properties were adopted (Table 1).

Table 1 - Structure properties

Members	h (m)	A (m ²)	I (m ⁴)	γ (KN/m ³)	E (MPa)	ν	ξ	
Ceiling Slab	1	0,8	0,86	0,0459	25	29870	0,2	0,05
Base	2	0,8	0,91	0,0485	25	29870	0,2	0,05
Walls	3	0,7	0,72	0,0294	25	29870	0,2	0,05
	4	0,8	0,88	0,0469	25	29870	0,2	0,05
Center columns	5	0,8	0,84	0,0448	25	29870	0,2	0,05
	6	0,4	0,16	0,0021	25	29870	0,2	0,05

2.6 Collapse analysis

The frame was designed based on the weight of the overburden soil, lateral earth pressure, and weight of the frame under ordinary loading conditions, but the earthquake load was not taken into account, which was the normal procedure used at that time for design.

However, to evaluate the damage with the model it's needed to introduce the horizontal and vertical accelerations (Fig. 8), resulting from seismic action. These data were recorded in some seismometers that were scattered in the central area of Kobe city. One of the most relevant records was recorded at Port Island, at a depth of 83 m and 3 Km away from station.

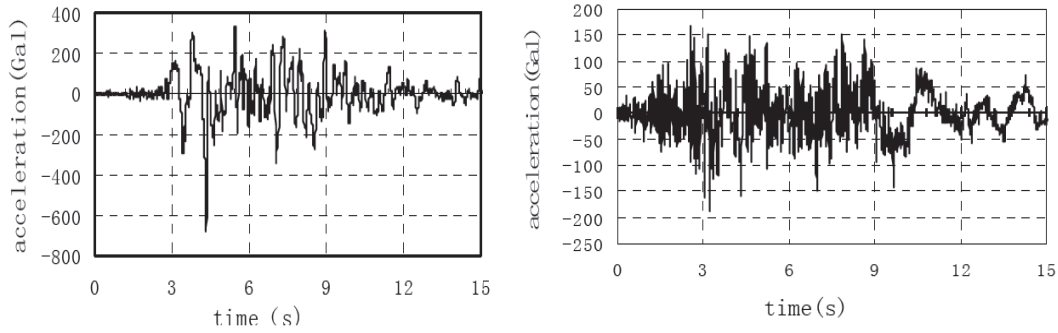


Fig. 8 - Input accelerations

Based on the observation of the damage to these columns and walls, the mechanism of the damage of the collapsed column in zone A is evaluated to be as follows (Yoshida and Nakamura, 1996): (1) - due to the strong horizontal component, the central column has reached its maximum capacity in the presence of bending moment and shear in the lower zone; the appearance and combination of these efforts is due to earthquake transverse component of the structure. (2) - in turn, their load carrying capacity was greatly reduced, so that the response to requests for vertical loads was nearly canceled entirely, unable to withstand the gravitational action.

3. Calibration of numerical model

One of the most intriguing problems for the geotechnical engineering complexity that presents is the prediction of the behavior and response of soil when subjected to seismic action.

3.1 Linear elastic analysis

These techniques are associated to the one-dimensional approach, considering that all layers are horizontal and that the response is predominantly caused by vertically propagation shear waves (Kramer, 1996).

The transfer function for uniform, damped soil on rigid rock is given by the next expression:

$$|F_2(\omega)| = \frac{1}{\sqrt{\cos^2 kH + (\xi kH)^2}} = \frac{1}{\sqrt{\cos^2\left(\frac{\omega H}{v_s}\right) + \left[\xi \frac{\omega H}{v_s}\right]^2}} \quad (1)$$

The frequencies that correspond to the local maxima are the natural frequencies of the soil deposit and its variable with the level of damping.

Natural frequencies for the soil deposit can be evaluated by:

$$f_n = \frac{(2n-1).V}{4H} \text{ (Hz)} \quad n = 1,2,3, \dots \quad (2)$$

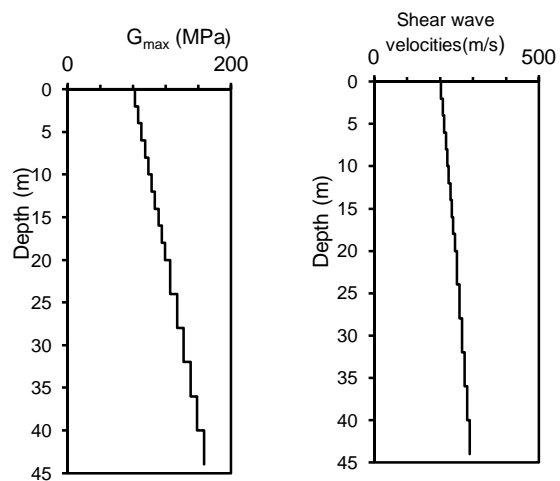


Fig. 9 - Profiles of the maximum shear stiffness and shear wave velocity

3.2 Equivalent linear method

The ground response analysis was performed using the equivalent-linear method with code EERA.

The code EERA considers the assumption of equivalent-linear visco-elastic soil behavior. The equivalent-linear model assumes that the shear modulus G and damping ratio ξ are function of the shear strain amplitude γ . The equivalent-linear analysis is repeated with updated values of G and ξ until those values are compatible with the effective shear strain induced in all the layers of the numeric model. Modulus reduction curve G/G_0 and variation of damping ratio ξ with shear strain level γ were defined according to typical results reported in the literature, as a function of PI. As the soil model consists of sand it's considered $PI=0$.

Ishibashi and Zhang (1993) developed an expression to determine the modules reduction curves, based on the plasticity index (PI) and the effective confining pressure. For the EERA code, and for a thickness of 44m for the layer, it was assumed a discretization of 2m for the first 10 layers and 4m for the others. Next, and according to 7 different levels of effective confining pressure it was made a correspondence between the layers and the modules reduction curve (Fig. 10).

According to Huo *et al* (2005), was considered $G_{max} = 80 MPa$ at the surface, increasing linearly to $167 MPa$ at a depth of 44 m in the bedrock layer (Fig. 9).

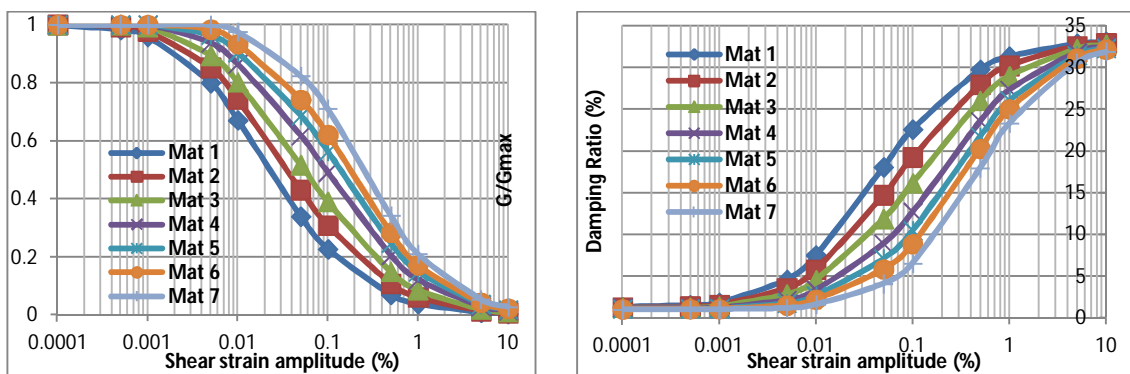


Fig. 10 - Modulus reduction curve and variation of damping ratio D with shear strain

3.3 SAP - Modal analysis

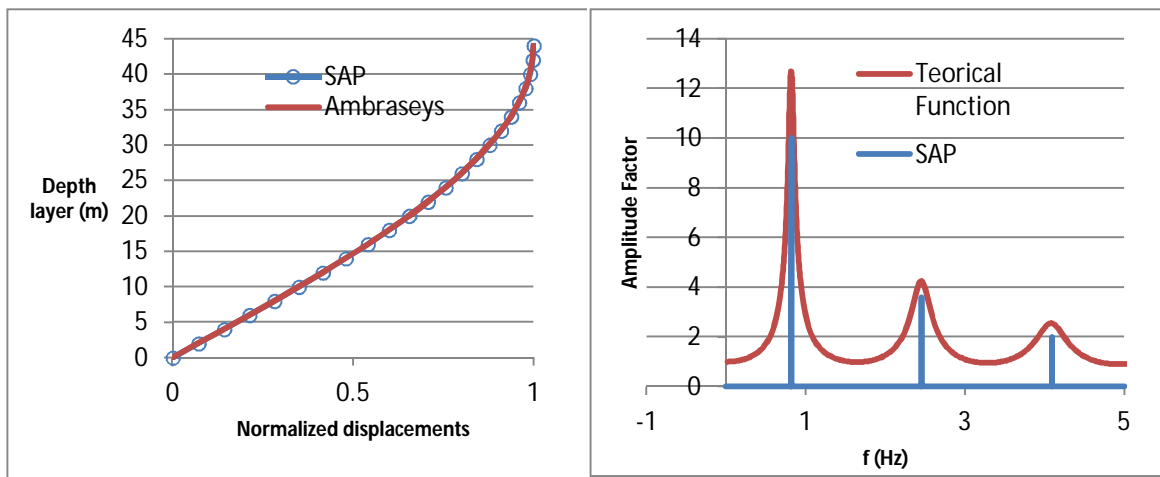


Fig. 11 - Validations with SAP2000

Two validations were performed using SAP2000. Firstly was compared for the first mode of vibration for the uniform soil layer, the offsets provided by the calculation program and the SAP solution Ambraseys (Fig. 11 - left). Second, it was tried to achieve whether there is a similarity between the theoretical model based on the hypothesis of vertically propagation shear waves and the transfer function obtained analytically from the response of the soil (Fig. 11 - right). Good agreement was achieved

3.4 Hardening Soil Model

The code PLAXIS was used and the Mohr-Coulomb failure criteria with hardening was adopted: "*Hardening Soil*" model. This model calculates the total strains using a stress-dependent stiffness, different for both virgin loading and un-reloading. The plastic strains are calculated by introducing a multi-surface yield criterion. Instead of using Hooke's single stiffness model with linear elasticity in combination with an ideal plasticity according to Mohr-Coulomb a new constitutive formulation using a double-stiffness model for elasticity in combination with isotropic strain hardening is presented.

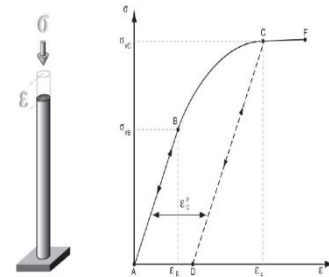


Fig. 12 - Behavior of the Hardening Soil model

In contrast to the perfectly elastic-plastic model, the yield surface of the "*Hardening Soil*" is not fixed in principal stress space, but it can expand due to plastic straining.

4. Modeling the station

The seismic soil-station interaction is studied in the time domain using the modal decomposition to seismic recording Island Port, Kobe.

Table 2 - Natural frequencies obtained with the program SAP

Comparing the dynamic properties in the case of model analysis homogeneous and stratified, it appears that the latter has much higher stiffness because the frequency of the fundamental mode is greater than twice the homogeneous model. It is also apparent that further modes of vibration were to be evaluated to obtain a summation of modal shares around 90% (Table 2).

Vibration mode	T	f	Mass participation in X direction	
	[s]	[Hz]	Individual (%)	Acumulated (%)
1 ^o	0,53	1,88	68,67%	68,67%
2 ^o	0,24	4,23	9,63%	78,53%
3 ^o	0,22	4,46	3,55%	82,07%
4 ^o	0,14	7,38	2,10%	84,81%
5 ^o	0,13	7,52	2,03%	86,84 %
6 ^o	0,09	10,38	2,86%	90,07%

As reference criteria for forces and according to the work of other authors it's possible to validate these. According to Huo *et al* (2005) the central column, due to static loads, has a level of axial force of 3700 KN result of static equilibrium. During the seismic action the axial force will be 4200 KN considering only the horizontal component of the action and 4900 KN taking into account both the horizontal and vertical action. The increased load from the static level to the dynamics due to the distortion which the structure is subjected by the vertical component and the inertial forces that are generated in the surrounding soil, especially the one that lies above it (Huo *et al*, 2005).

Regarding the finite model achieved the axial force in the center column obtained is about 2799 KN and 3700 KN in the model developed by Huo *et al* (2005). This difference can be easily explained by the different models existing in both cases. While in this work was adopted a model in which the properties of mass and stiffness differ in each layer, these authors intended to vary the stiffness and admit always the same density for the soil.

An *et al* (1997) indicates that the shear capacity and the ductility of the central column are the most important parameters which influence the seismic performance.

Based on the interaction N-M curve (Fig. 13) according to the section in central columns presented, it is observed that for static load (weight of the structure itself and the weight of soil above) this is a level of acceptable resistance. Forces computed with SAP model at the base of the central column when combining the static action with the horizontal accelerogram of Kobe are the same in terms of axial force (N = 2799 KN), with an addition of large bending moment (M = 1220 KN.m). The combination of these two structural forced makes the point of dynamic action in Fig. 13 goes outside the area bounded by the curve of interaction. This demonstrates that the axial static was not the cause of the rupture of the column, but the binomial between axial and bending moment (Yubin and Rushin, 2008).

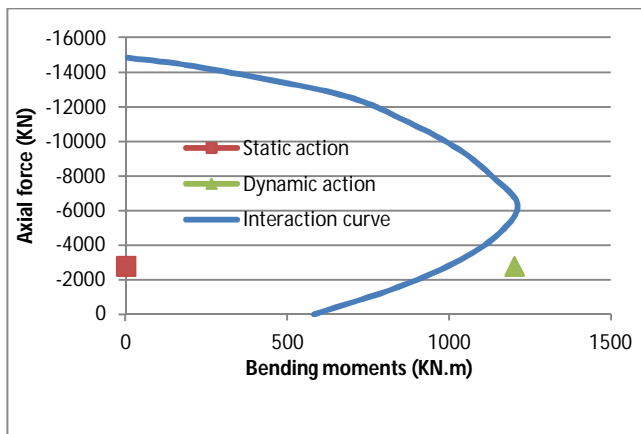


Fig. 13 - Interaction curve for N-M

According An *et al* (1997), associated with the failure mechanism, the distortion value for the central column it's around 1.5%. Using the SAP model it can be obtained a value of distortion of 1.53%, very close to the one that's indicated by references. It appears therefore that for both models, with this limit value as distortion, collapse mechanism can be associated with a lack of ability to withstand relative displacement.

5. Sensitivity study

In this chapter it will be analyze the influence that the construction process can have on the system response to seismic action or to static forces, the latter being one of the most important actions to be taken into account on the design of such underground structures. It will be used the finite element program PLAXIS.

To perform the modeling was indispensable the resource program EERA. Necessary elements are obtain so that the analysis takes into account the degradation of soil stiffness properties with the seismic action, such as stiffness in each soil layer and damping ratio.

Viscous damping is introduced here by means of the Rayleigh formulation, whose damping matrix is defined as follows:

$$[C] = \alpha[M] + \beta[K] \quad (3) \quad \{\alpha; \beta\} = \left\{ \frac{5}{3} \times \xi \times \omega_1; \frac{1}{3} \times \frac{\xi}{\omega_1} \right\} \quad (4)$$

where $[M]$ and $[K]$ are the mass and stiffness matrix of the Rayleigh system, respectively.

Although, in case of visco-elastic layers the Rayleigh coefficients may be calibrated according to the ratio damping and the angular frequency of the first vibration mode ($8,85 \text{ rad/s}$) by the relation defined in (4).

The boundary conditions adopted for the static stages were the standard ones: nodes at the bottom of the mesh were fixed in both vertical and horizontal direction. In the dynamic analyses, the bottom of the mesh was assumed to be rigid and the lateral sides were characterized by the viscous boundaries proposed by Lysmer and Kuhlmeyer, with parameters $a=1.0$ and $b=0.25$.

The mesh employed in the present study is reported in Fig. 14: it's characterized by a width (352m) equal to eight times its height (44m), in order to minimize the influence of boundary conditions on the computed results. The domain was discretised in a total of 1702 15-node plane strain triangular elements. In the central part the mesh was refined to take account a more accurate model. Like the 1D ground response analyses, the domain was partitioned into 16 layers to account variable stiffness and damping parameters with the depth.

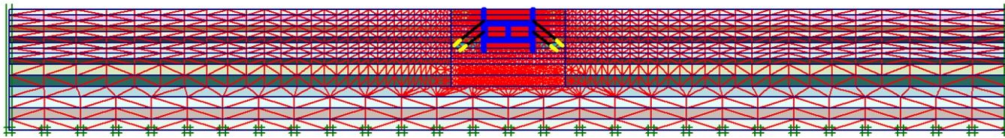


Fig. 14 - Mesh employed in the FE analyses

Three models were studied: model 1 – retaining walls but without simulation of construction; model 2 - retaining walls with the simulation of construction; model 3 - without retaining walls.

The analyses of these models lead to the following conclusions:

- the magnitude the displacements and bending moments diagram are larger in model 2;
- plastic points appear in greater number in the model 2, at the base of the excavation and at the surface level, near the walls;
- due to seismic action, the residual displacements in the retaining wall are a slightly higher in model 2, due to a large number of plastic points that occur in this model;
- bending moments in the walls are 42% larger in model 2 comparing with model 1, for static action;
- tie back walls change the forces that appeared in the station structure, comparing all models. For the central column, higher bending moment occurred in model 3. The presences of walls restrict the relative movements of the station when the seismic action is activated.

6. Concluding remarks and future perspectives

Main conclusions:

- was identified the mechanism of collapse for the station. Due to the strong horizontal shaking, the central column has reached its maximum capacity in the presence of bending moment and shear in the lower

zone. The column was not designed to withstand the displacements imposed by the ground, denoting lack of ductility and flexibility.

- the application of code EERA was used to take into account the nonlinear behavior of soil due to seismic action. The stiffness and damping computed for each layer was used in PLAXIS model.
- With the modal analysis (SAP) was intended to characterize the seismic response of the system. It was found that the failure in the central column occurs due to the presence of bending moment and axial force.
- In the sensitivity study various parameters were modeled in the observed models. The most notable differences relate to design values and displacements in the structure elements (central column and walls) and location of plastic points in the mesh according to the analyzed model.

There are some changes and studies that could be done to consolidate the tendencies here presented.

- Comparison of available results in the literature obtained by simulating the station collapse in shaking table;
- Assess the influence of the geometry of the tunnel, depth and position of the columns in the seismic response of the structure;
- Analyze with the seismic rules implemented in Portugal if the Daikai station, before the collapse, was well design.

7. Bibliography

"The January 17, 1995 Kobe Earthquake - An EQE Summary Report". San Francisco, USA.

Huo, H.; Bobet, A., Fernández, G., & Ramírez, J. (2004). "Load Transfer Mechanisms between Underground Structure and Surrounding Ground: Evaluation of the Failure of the Daikai Station" *Journal of geotechnical and geoenvironmental engineering*, ASCE, Vol. 131, No. 12, pp.1522-1533.

Iida, H.; Hiroto, T.; Yoshida, N.; & Iwafuji, M.(1996). "Damage to Daikai Subway Station". *Special Issue of Soils and Foundations*, pp. 283-300.

Kobe City (1980). *Ground in Kobe, Kobe city*.

Yoshida, N.; Nakamura, S., (1996). "Damage to Daikai subway station during the 1995 Hyogoken-Nunbu earthquake and its investigation". *Eleventh World Conference on Earthquake Engineering*, Paper No. 2151.